JEODEZİ VE JEOİNFORMASYON DERGİSİ
JOURNAL OF GEODESY AND GEOINFORMATION
ISSN : 2147-1339
e-ISSN: 2667-8519

Araştırma Makalesi / *Research Article*
Yıl / *Year:* 2025 **Cilt** / *Volume:* 12 **Sayı** / *Issue*: 1
Sayfa / *Page*: 1-19
Dergi No / *Journal No*: 121
Doi: 10.9733/JGG.2025R0001.E

Assessment of GNSS-IR performance using multi-GNSS and multi-frequency SNR data from smartphones

Cemali Altuntas[1*], Nursu Tunalioglu[1]

[1]*Yildiz Technical University, Campus of Davutpaşa, Faculty of Civil Engineering, Department of Geomatic Engineering, Esenler, Istanbul, Türkiye.*

Abstract: *Smartphones are equipped with embedded Global Navigation Satellite Systems (GNSS) chips that support multiple satellite systems, enhancing precision in positioning, navigation, and timing services. The introduction of GNSS Interferometric Reflectometry (GNSS-IR) leverages these capabilities by analyzing multipath signals and reflections to estimate surface properties more accurately. Given their multi-GNSS and multi-frequency capabilities, along with lower cost and greater portability compared to traditional geodetic receivers, smartphones hold significant potential for application in GNSS-IR technologies. In this study, we conducted a three-day experimental evaluation, observing for six hours each day to assess the accuracy of reflector height and change estimations from multi-frequency multi-GNSS SNR data provided by geodetic receivers and smartphones. The setup included two CHC i90 Pro geodetic receivers and two Samsung Galaxy Note 20 Ultra smartphones, positioned in both zenith-looking and nadir-looking orientations, facilitated by an experimental setup developed under TÜBİTAK project number 121Y348. Our analysis focused on the number of valid estimations, peak-to-background noise ratio (PBNR) values, and the accuracy of reflector height and height difference estimations with satellite-based and frequency-based assessments. According to the results, geodetic receivers consistently outperform smartphones in data collection stability for GNSS-IR applications. We also found that the platform orientation of smartphones (flat, inverted, or inclined) has a minimal impact on the accuracy of GNSS-IR estimations, and the most reliable smartphone data is obtained from GPS satellites. Furthermore, using signals with wavelengths shorter than 20 cm in smartphone-based GNSS-IR studies provides better results and offers a cost-effective method for long-term monitoring of climatological parameters such as snow depth, sea level, and vegetation height.*

Keywords: Multi-GNSS, Multipath, GNSS-IR, SNR, Smartphone

Akıllı telefonların çok frekanslı çoklu-GNSS SNR verilerinin GNSS-IR performansının değerlendirilmesi

Öz: *Akıllı telefonlar, birden fazla uydu sistemini destekleyen gömülü Küresel Navigasyon Uydu Sistemleri (GNSS) çipleri ile donatılmıştır. Bu durum konum belirleme, navigasyon ve zaman ölçümü çalışmalarında doğruluğu artırmaktadır. GNSS İnterferometrik Reflektometri (GNSS-IR) yöntemiyle, bu özelliklerden faydalanılarak yüzey özelliklerini daha doğru kestirmek için çok yolluluk etkisindeki sinyallerin ve yansımaların analizi gerçekleştirilebilmektedir. Çok frekanslı çoklu-GNSS veri toplama kabiliyetine sahip olmalarının yanı sıra, geleneksel jeodezik alıcılara kıyasla daha düşük maliyetli ve taşınabilir olmaları nedeniyle akıllı telefonlar, GNSS-IR çalışmalarında uygulama için önemli bir potansiyele sahiptir. Bu çalışmada, jeodezik alıcılar ve akıllı telefonlardan sağlanan çok frekanslı çoklu-GNSS SNR verilerinden elde edilen reflektör yüksekliği ve yükseklik değişimine ilişkin kestirimlerin doğruluğunu değerlendirmek için her gün altı saatlik ortak gözlem içeren üç günlük bir deneysel çalışma gerçekleştirilmiştir. 121Y348 numaralı TÜBİTAK projesi kapsamında geliştirilen deney düzeneğine, iki CHC i90 Pro jeodezik alıcı ve iki Samsung Galaxy Note 20 Ultra akıllı telefon, başucu ve ayakucu doğrultularına bakacak şekilde yerleştirilmiştir. Geçerli kestirim sayısı, pik-arka plan gürültü oranı değerleri, reflektör yüksekliği ve yükseklik değişimi kestirimlerinin doğruluğu üzerinden uydu sistemi ve frekans temelli değerlendirme yapılmıştır. Bulgular, jeodezik alıcıların GNSS-IR uygulamalarında veri toplama stabilitesi yönünden akıllı telefonlardan daha üstün performans sağladığını göstermiştir. Ayrıca, akıllı telefonların yöneliminin (düz, ters veya eğimli) GNSS-IR kestirimlerinin doğruluğu üzerindeki etkisinin çok az olduğu ve en stabil akıllı telefon verilerinin GPS uydularından elde edildiği görülmüştür. Buna ek olarak, 20 cm'den kısa dalga boyuna sahip sinyallerin akıllı telefon tabanlı GNSS-IR çalışmalarında kullanılmasının daha iyi sonuçlar sağladığı ve kar kalınlığı, deniz seviyesi ve bitki yüksekliği gibi iklimbilimsel parametrelerin uzun vadeli izlenmesi için düşük maliyetli bir alternatif teşkil ettiği tespit edilmiştir.*

Anahtar Sözcükler: Çoklu-GNSS, Çok yolluluk, GNSS-IR, SNR, Akıllı telefon

* Sorumlu Yazar/Corresponding Author: Tel: +90 212 383 5309

Geliş Tarihi/Received: 11.05.2024
Kabul Tarihi/Accepted: 16.07.2024

0000-0002-9660-6124, cemali@yildiz.edu.tr (Altuntas C.)*
0000-0001-9345-5220, ntunali@yildiz.edu.tr (Tunalioglu N.)

1. Introduction

The number and usage rate of portable and wearable mobile technological devices such as smartphones, tablets, and smartwatches, as well as the interest in innovative applications and designs involving these devices, are increasingly growing. In the 21st century, smartphones, in particular, are actively used as personal assistants to many people. Smartphones offer versatile and useful features, considering their ability to provide mobile internet access, voice/video calling services, execute various sensor-based applications, deliver quick solutions for positioning, navigation, and timing (PNT) with Global Navigation Satellite Systems (GNSS), and their easy portability. Consequently, the economic market size of smartphones is considerably larger compared to other mobile devices. According to the European GNSS Agency (GSA) 2019 Market Report, the number of smartphone users worldwide is projected to reach 3.5 billion by the end of 2020 (GSA, 2019). Also, according to the European Union Agency for the Space Program (EUSPA) Earth Observation (EO) and GNSS Market Report 2024, the annual shipments of GNSS devices are forecasted to rise from 1.6 billion units in 2023 to 2.2 billion units in 2033, with Consumer Solutions (such as smartphones, fitness devices, and tablets) and Road and Automotive (including in-vehicle systems and various types of on-board units) accounting for the majority of the shipments by 2033 (EUSPA, 2024). The significant potential for use and the advantages in terms of mobility have recently enabled the use of smartphones in engineering measurement applications as well. Moreover, these devices are now equipped with GNSS chips, LiDAR, accelerometers, and other sensor-based enhancements and software, enabling various engineering applications.

Smartphones contain a variety of sensors, among which the embedded GNSS chips are crucial. These modular chips, which integrate receiver and antenna structures, provide PNT services at various accuracy levels, and are incorporated into smartphones along with other sensors. Initially, GPS chips were first added to smartphones in 1999. However, modern smartphones now support multi-GNSS systems, including GPS, GLONASS, Galileo, BeiDou, QZSS, and SBAS, enhancing positioning capabilities. A significant development occurred in May 2016 when Google announced at the I/O 2016 conference that with Android 7.0 (Nougat), it would open access to raw GNSS data collected by smart devices. This move facilitates the processing of raw GNSS data, using code, carrier phase, and Doppler observations from satellites, which has opened opportunities for research into sub-meter level positioning accuracy (Banville & van Diggelen, 2016). Another significant step forward in GNSS positioning for smartphones occurred in May 2018 with the introduction of the Mi8 by Xiaomi, the world's first dual-frequency smartphone. The Xiaomi Mi8 is equipped with the Broadcom BCM47755 embedded GNSS chip, capable of recording signals from GPS L1/L5 and Galileo E1/E5a. This model also supports single-frequency signals from GLONASS, BeiDou, and QZSS. This development marked the beginning of achieving centimeter-level accuracy in positioning with smartphones, fundamentally changing research into precision positioning with mobile devices. By offering a cost-effective alternative to expensive geodetic receivers, it has led to numerous studies on the usability of affordable smartphones in engineering applications (Robustelli et al., 2019).

One of the fundamental differences between geodetic GNSS receivers and smartphone GNSS chips lies in the characteristics of the antennas used. Geodetic antennas typically use circular polarization, while smartphone GNSS chip antennas have linear polarization. This difference makes the smartphone GNSS antennas more susceptible to the multipath effects of GNSS signals reflected from nearby surfaces. As a result, smartphone GNSS antennas generally collect lower quality GNSS measurements compared to geodetic GNSS receiver antennas, which are designed to minimize multipath effects, creating a disadvantage for smartphone based GNSS positioning. However, a method known as GNSS Interferometric Reflectometry (GNSS-IR), utilized for approximately the last 15 years, takes advantage of these unwanted multipath signals for precise positioning by analyzing the oscillations they cause in signal strength. This analysis allows determining the geometric and radiometric characteristics of the reflective surfaces. The additional path created by the reflected signal can introduce errors of up to a meter in precise positioning. Still, since the power of the multipath-affected signal is related to the geometry between the antenna phase center (APC) and the reflective surface, this data is valuable for estimating the vertical distance between the APC and the ground. The data indicating signal strength, typically presented as the carrier-to-noise density ratio (C/N0) or signal-to-noise ratio (SNR), is provided to users by receivers and smartphones. SNR-based GNSS-IR has been effectively used to determine climatological parameters such as soil moisture (Altuntas & Tunalioglu, 2020; Chew et al., 2013; Larson et al., 2008), snow depth (Larson et al., 2009; Nievinski & Larson, 2014; Tunalioglu et al., 2019), and sea level (Altuntas & Tunalioglu, 2023; Besel & Kayikci, 2021; Hu et al., 2021; Larson et al., 2013; Williams et al., 2020).

In the first study to examine the altimetric performance of the GNSS-IR method using SNR data from mobile devices, Strandberg and Haas (2019) analyzed SNR data from the GTGU GNSS station located at the Onsala Space Observatory in Sweden and from a Samsung Galaxy Tab A 10.1 4G tablet. They correlated the estimated reflector heights with sea level measurements. The sea level values were validated with tide gauge measurements located a few meters from the GNSS station. The RMSE (Root Mean Square Error) between the sea level estimates derived from the GNSS station and tablet data, and the tide gauge measurements obtained as 6.2 cm. The study also noted that the tablet provided only L1 frequency data, resulting in a significantly lower number of valid estimates throughout the study period compared to a geodetic receiver capable of handling L1, L2, and L5 frequencies. Altuntas and Tunalioglu (2021) conducted an experimental study in which they analyzed multi-GNSS SNR data obtained from a Xiaomi Mi8 Lite smartphone, and a Trimble NetR9 geodetic receiver connected to a TRM57970 geodetic GNSS antenna. Over a period of three days, measurements were taken for five hours each day to assess the accuracy of reflector height estimations. The study found that the RMSE values were 1.9 cm for the smartphone and 3.7 cm for the geodetic antenna when compared to in-situ measurements. Liu et al. (2022) evaluated the altimetry performance using multi-GNSS SNR data collected from a Huawei P30 smartphone, which was paired with a low-cost antenna-equipped u-blox F9P receiver. In their study, which analyzed 20 days of data, it was found that the GPS L1, GLONASS G1, and BDS B1I frequencies provided precise and stable reflector height measurements. However, the performance of GPS L5 and Galileo E5a was somewhat lower. Chen et al. (2023) assessed the performance and feasibility of low-cost GNSS devices for temporary sea level measurements. The study utilized several devices, including a Redmi Note 9 Pro smartphone connected to a BT560 antenna and a CHCNAV P5 GNSS receiver, alongside another receiver with a standard geodetic-quality antenna and a pressure tide gauge for comparison. After collecting and analyzing over 80 hours of SNR data from various GNSS constellations, the research concluded that low-cost GNSS devices could provide stable sea level measurements with a RMSE of approximately 16 cm, which is comparable to, or even slightly better than, that of traditional geodetic-quality devices. Zheng and Chai (2023) investigated the accuracy of ground height retrieval using GNSS-IR technology. The study involved Hi-Target geodetic GNSS receivers, an Honor 60 smartphone, and a Huawei MatePad Pro tablet to collect data over five days, with antenna heights ranging from 0.8 m to 1.6 m. It was found that a linear relationship could be established between the inversion error and antenna height, with an RMSE for smart devices at 4.7 cm and 4.2 cm, compared to 1.0 cm for geodetic GNSS receivers. The RMSE values mentioned pertain to the performance of both smartphones and GNSS receivers under varying antenna height conditions, indicating the height estimation error for each device over the range of station heights.

Considering existing studies on GNSS-IR with mobile devices, it appears that there is no comprehensive evaluation in the literature of Android-based smartphones equipped with dual-frequency multi-GNSS chips across different frequency ranges and constellations. In this study, an experimental evaluation was conducted over three days, with six hours of observation daily, aiming to assess the accuracy of reflector height estimations derived from dual-frequency multi-GNSS SNR data provided by smartphones, based on varying reflector heights and receiver orientations. The setup included two CHC i90 Pro geodetic receivers and two Samsung Galaxy Note 20 Ultra smartphones, arranged in both zenith and inverted orientations.

Changes in height and orientation were facilitated by an experimental setup developed under the TÜBİTAK project number 121Y348. The results were analyzed based on the number of valid estimations, peak-to-background noise ratio (PBNR) values, and accuracy of reflector height and reflector height difference estimations.

2. SNR Based GNSS-IR

The signals transmitted by GNSS satellites are subject to various effects caused by interactions with atmospheric layers such as the ionosphere and troposphere, as they travel to the receiver antenna. One significant impact these signals face is the multipath effect, which occurs when the signal transmitted from the satellite reflects off one or more surfaces until it reaches the receiver. In ground based GNSS measurements where multipath effects are present, the signals coming directly from the satellite and those reflected from nearby surfaces interfere at the APC of the receiver, resulting a composite signal. Although this composite signal is a challenging source of error in positioning applications, it provides an alternative opportunity to determine the geometric and radiometric characteristics of the reflected surface when analyzed using a method known as GNSS-IR.

GNSS receivers not only provide phase information of the signal but also code measurements and navigation messages, as well as the power and noise of the signal. GNSS antennas detect signals emitted by GNSS satellites, and these signals are then processed by GNSS receivers. The signal strength, usually expressed as $\mathrm{C/N_0}$, can be converted to SNR assuming a noise bandwidth of 1 Hz (Larson & Nievinski, 2013). SNR is composed of trend and harmonic components of direct and reflected signals due to interference and antenna gain pattern (AGP):

$$SNR = tSNR + dSNR \tag{1}$$

where $tSNR$ denotes the trend of the SNR signal and $dSNR$ denotes the detrended SNR signal. The $tSNR$ is largely dependent on the AGP of the receiver and can be modeled and extracted using a polynomial of second degree or higher. The $dSNR$ signal, obtained after the trend is removed, has a periodic nature and can be expressed as follows (Larson et al., 2008):

$$dSNR = A\cos\left(\frac{4\pi h}{\lambda}\sin\varepsilon + \phi\right) \tag{2}$$

Here, A and ϕ represent the amplitude and phase of the $dSNR$ signal, respectively, h denotes the vertical distance between the APC and the reflected surface (i.e., reflector height), λ denotes the wavelength of the GNSS signal, and ε indicates the satellite elevation angle. Since $\sin\varepsilon$ is the independent variable of the $dSNR$ signal, the following relationship exists between the dominant frequency (f) of the $dSNR$ signal and the reflector height:

$$h = \frac{f\lambda}{2} \tag{3}$$

Since $\sin\varepsilon$ is the sine of the satellite elevation angle, it is irregularly sampled. Therefore, in this study, the Lomb-Scargle Periodogram (LSP) analysis, commonly used for irregularly sampled data, was used to find the dominant frequency of the $dSNR$ signal (Lomb, 1976; Scargle, 1982). The dominant frequency values were then converted into reflector heights using Equation (3).

3. Materials and Methods

This section begins by introducing the study area and the setup developed for the experimental study under the project. It then proceeds with preliminary analysis steps to determine appropriate parameters for the azimuth range, satellite elevation angle range, and minimum PBNR condition, followed by further analysis procedures.

3.1 Study Area and Experimental Design

The study area is located within the Yıldız Technical University's Davutpaşa Campus in Istanbul, Turkey (Figure 1). The primary reason for selecting this area was its capacity to provide extensive views along the southeast and southwest lines and to offer a surface with low roughness, which helps eliminate topographical effects that could impact the study results. The study area measures approximately 90 m x 140 m. The experimental study involved collecting measurements for two 3-hour periods each day on the 283rd, 284th, and 286th days of the year (DoY), October 10, 11, and 13, 2022, conducting a 3-day experiment.

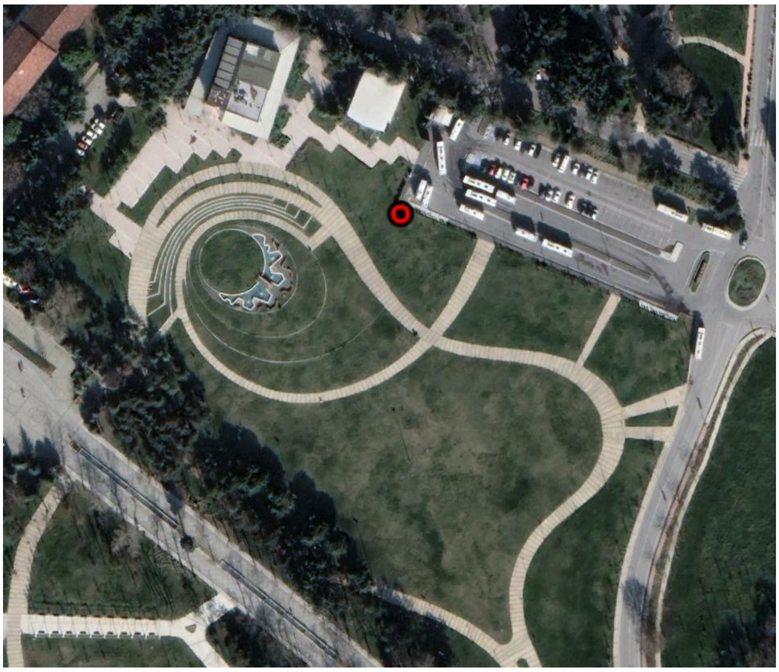

Figure 1: *Study area*

In the conducted experiment, two CHC i90 Pro geodetic receivers and two Samsung Galaxy Note 20 Ultra smartphones were used. The receivers and smartphones were set up with (1) a 20% incline on the first day, (2) a -20% incline on the second day, and (3) a 0% incline (i.e., standard orientation) on the third day (Figure 2). Here, the positive and negative inclines refer to the tilt observed when viewing the platform from the side, with the azimuth direction on the right-hand side. One of the aims of this experiment was to determine the effects of these inclinations on the estimation of SNR metrics. The receivers and experimental setup were oriented towards a 160° azimuth for all three days to face the smooth surface of the terrain. Observations were carried out daily between 09:30 and 15:30 local time (UTC+3). After three hours of observation each day, the reflector heights were decreased by 10 cm, and the remaining three hours of observation were conducted at these reduced reflector heights. The in-situ reflector heights obtained by measuring the Antenna Reference Point (ARP) heights are provided in Table 1.

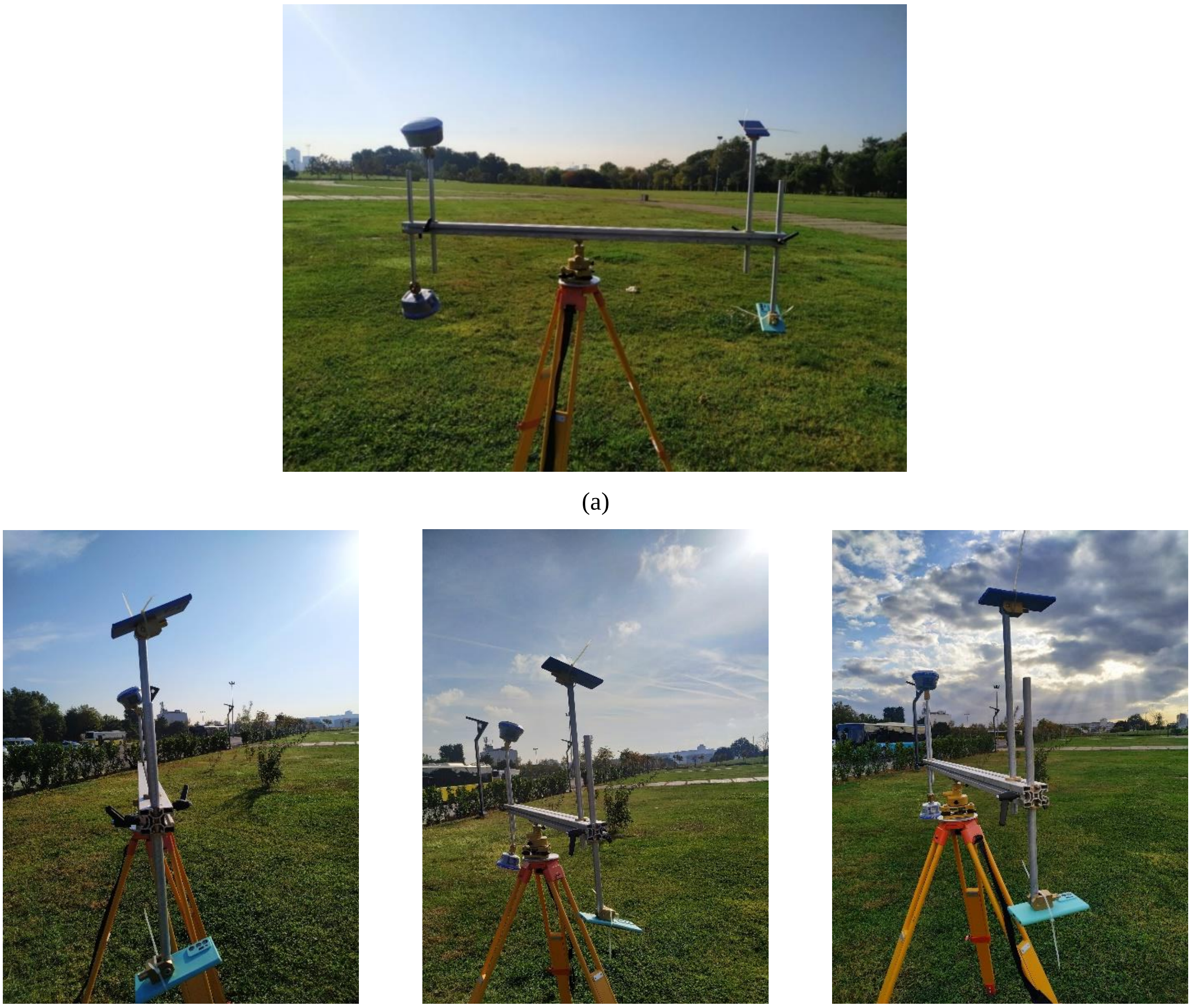

(a) (b) (c) (d)

Figure 2: *(a) General view of the experimental setup and the inclinations applied to the receivers in the setup for three separate days (b) Day 1: October 10, 2022 (20%), (c) Day 2: October 11, 2022 (-20%), (d) Day 3: October 13, 2022 (0%)*

Table 1: *In-situ reflector heights found by adding the offset values from the NGS antenna calibration report to the ARP heights*

Receiver		Day 1 (DoY: 283)	Day 2 (DoY: 284)	Day 3 (DoY: 286)
CHC1	Reflector height (first 3 h) (m)	1.910	1.965	1.990
	Reflector height (last 3 h) (m)	1.820	1.860	1.885
CHC2	Reflector height (first 3 h) (m)	1.135	1.135	1.170
	Reflector height (last 3 h) (m)	1.090	1.015	1.065
SP01	Reflector height (first 3 h) (m)	1.945	1.940	1.940
	Reflector height (last 3 h) (m)	1.845	1.845	1.840
SP02	Reflector height (first 3 h) (m)	1.260	1.240	1.240
	Reflector height (last 3 h) (m)	1.160	1.140	1.140
	Orientation	20%	20%	-20%

3.2 Preliminary Design

The analysis was conducted in two stages. During the preliminary analysis phase, general evaluations were made and appropriate criteria for further analysis were determined. The second stage aimed to develop final results by implementing strategies based on the outcomes of the first stage. In the preliminary analysis phase, a 0°-360° azimuth range was used to assess signals coming from all directions. A satellite elevation angle range of 5°-25° was chosen. The minimum satellite elevation angle range condition was set at 10°, and the minimum PBNR condition was set at 3. Since the reflector heights were decreased by 10 cm after the first three hours of observation each day, the analysis results were evaluated separately for the first three hours and the last three hours.

3.2.1 Suitability of the Azimuth Range

Since no azimuth mask was applied, the initial evaluation focused on determining the suitability of the azimuth range used. Data obtained during the first three hours of the first day of the experiment were analyzed to estimate reflector heights. Since the heights of the receivers varied, the median reflector height for each receiver was calculated, and the deviation of each estimate from its median value was computed. The variation of these differences according to azimuth is shown in Figure 3.

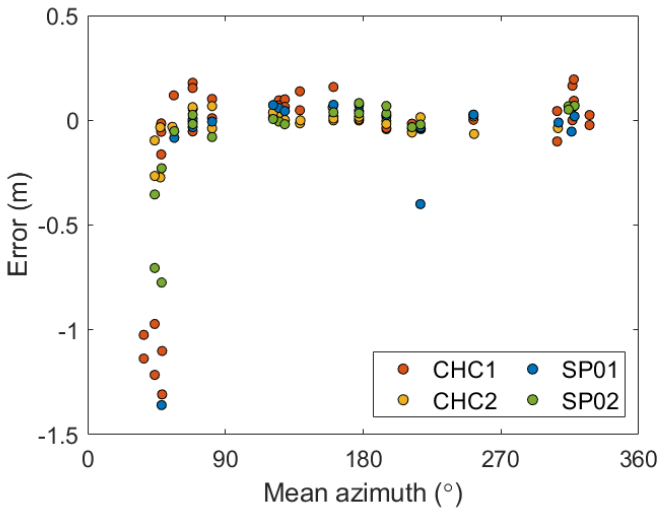

Figure 3: *Variation of estimation errors with azimuth*

According to Figure 3, it is evident that data with an average azimuth value below 45-50° tend to result in worse reflector height estimates. The main reason for this appears to be that the surface in these azimuth directions is not sufficiently wide and smooth. Considering that the average azimuth width for the visualized data is 10.5°, using an azimuth range of 60°-360° instead of 0°-360° would exclude estimates with high errors due to azimuth-related factors. Therefore, an azimuth range of 60°-360° will be applied in the further analysis phase.

3.2.2 Minimum Satellite Elevation Angle Range Width Condition

Accurate estimation of SNR metrics requires sufficiently long data for each satellite pass, but there is no widely accepted standard for this in the literature. The oscillations in SNR data caused by multipath are directly related to the reflector height; a higher reflector height increases the frequency of SNR oscillations, while a lower one decreases it. Detrended SNR data, when lacking sufficient waveforms, results in lower spectral resolution of frequency estimation. The amount of wave contained in the $dSNR$ data is a function of the sine of the satellite elevation angle, and thus varies more with the range of satellite elevation angles than with time. To illustrate this effect, S1C signal data from satellite G27 received by a smartphone (SP01) on the first day of the experiment was analyzed. This SNR data was detrended using a third-degree polynomial. Reflector height estimates, PBNR values, and LSP peak widths (PW) for different satellite elevation angle ranges and widths are given in Table 2, and the data and LSP graphs are shown in Figure 4. Here, the PBNR value is the ratio of the LSP peak spectral amplitude to the average spectral amplitude, while the LSP peak width is the width of the peak at half its maximum spectral amplitude value, and the term “error” refers to the difference between the single reflector height estimate and the in-situ value for a selected satellite, and its specific $dSNR$ data.

Table 2: *Reflector height (RH) estimates, estimation errors, PBNR values, and LSP PW values obtained using different satellite elevation angle ranges and range widths for the G27 S1C signal collected by the smartphone SP01 on DoY: 283*

Range (°)	Range width (°)	RH (m)	Error (cm)	PBNR	PW (m)
5-25	20	1.960	1.5	6.78	0.336
5-20	15	1.977	3.2	5.71	0.444
5-15	10	1.934	-1.1	4.11	0.669
5-10	5	2.017	7.2	2.84	1.258
10-25	15	1.949	0.4	5.51	0.457
10-20	10	1.954	0.9	3.91	0.709
10-15	5	2.427	48.2	2.26	1.287
15-25	10	1.941	-0.4	4.46	0.764
15-20	5	2.130	18.5	2.82	1.399
20-25	5	2.520	57.5	2.35	2.011

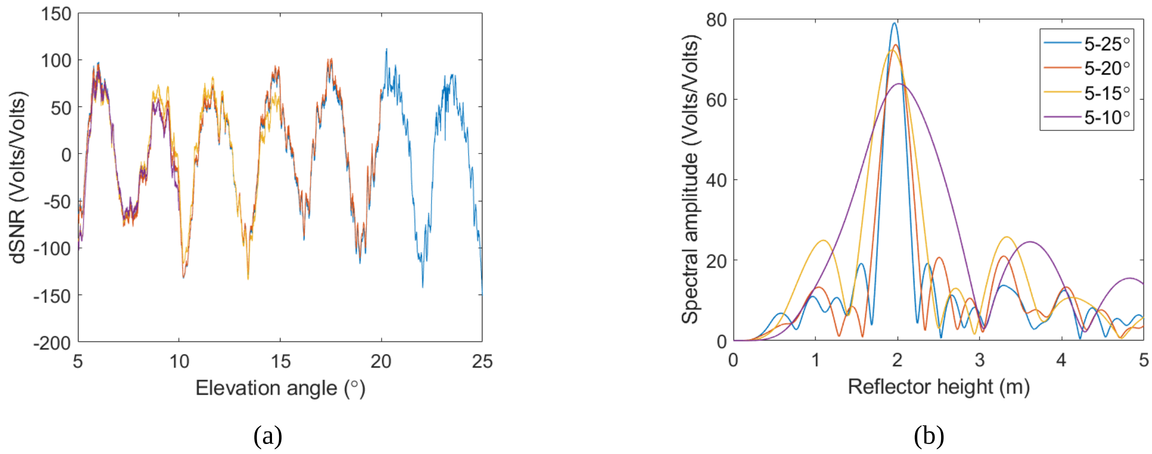

Figure 4: *(a) dSNR data and (b) LSP graphs for different satellite elevation angle ranges of the G27 S1C data collected by the smartphone SP01 on DoY: 283*

Considering the values in Table 2, it is seen that reducing the range width increases estimation errors, decreases PBNR values, and increases PW values. The PW value is inversely proportional to the spectral resolution of the frequency; therefore, an increase in PW value reduces the reliability of the estimates. PBNR value is widely used in literature for determining good reflector heights and is expected to exceed a certain threshold. Thus, a low PBNR value indicates a weak and/or noisy $dSNR$ signal, leading to less accurate estimates. Overall, the results in Table 2 show that when the range width is 10°, 15°, and 20°, estimation errors are below 4 cm, PBNR values are above 3, and PW values are below 0.8 m.

Figure 4 displays an example of a $dSNR$ data with strong reflection. As the range width decreases, the full wave count drops from 7 to 2. Consequently, the peaks in the LSP graph widen, increasing the uncertainty of the estimates. Considering that the sample data in Figure 4 is one of the best series among the data, reducing the range widths not only increases peak widths but also leads to higher errors in reflector height estimates. Keeping the minimum satellite elevation angle range width at the maximum (20° for this analysis) would exclude many data points, significantly reducing the number of estimates. Therefore, based on these results, a 10° value has been chosen to be applied as the minimum range width condition, ensuring an acceptable level of error (<4 cm) and a higher number of estimates.

3.2.3 Minimum PBNR Condition

The PBNR value is the ratio of the maximum amplitude in the LSP to the background noise. It is commonly used as a quality control criterion for signals in the literature. This is because having a strong amplitude alone may not suffice for determining the frequency of a signal. High amplitude values become insignificant if the signal is interfered with by other signals of different power and frequency or if the noise level is high. Therefore, the strength of a signal in terms of frequency discrimination is measured not by the level of its amplitude alone, but by its level relative to the background noise. Although the minimum PBNR ratio is conventionally chosen as 4 in the literature, there are studies where it is used as 2, 2.5, or 3, depending on the data or the characteristics of the terrain surface (Altuntas et al., 2022).

In the experimental study conducted, receivers were subjected to both positive and negative 20% inclinations. It is known that the AGP of geodetic receivers is designed to receive signals from low satellite elevation angles with lower gain. The impact of multipath in the SNR data of a geodetic receiver set up on a flat platform is predominant up to 25° to 30°. When the receiver platform is inclined positively, multipath-induced oscillations will be weaker or less frequent in the direction of the azimuth to which the platform is oriented. In this case, it would be inappropriate to require a minimum PBNR of 4 for data from a standard setup geodetic receiver. Therefore, for appropriate comparison of data across different days, using a threshold value of 3, as used in the literature, would be more suitable.

3.3 Further Analysis

In the further analysis phase, evaluation strategies suitable for the station are applied based on the results from the preliminary analysis. Here, a common evaluation strategy has been implemented for both geodetic receivers and smartphones. The degree of the polynomial used to remove the trend in the SNR data was chosen as 5 to eliminate possible low-frequency components. The analyses utilized a satellite elevation angle range of 5°-25° and an azimuth range of 60°-360°, and the data provided by the receivers and smartphones were evaluated to include all satellite systems and frequencies. The results obtained with this analysis strategy are examined in detail for different satellite systems and frequencies in the following section.

4. Results and Discussion

4.1 Satellite System Based Assessment

All receivers used in the study have the capability to collect data from four constellations (GPS, GLONASS, Galileo, BeiDou). Signals from different satellite systems can be distinguished by technical characteristics such as frequency, power, and modulation. Therefore, a satellite system-based analysis is necessary to assess the performance of these systems. The analysis was conducted to include results from two strategies: one where PBNR and minimum satellite elevation angle range width conditions were not applied, and another where they were applied. Scenarios where conditions are applied are labeled as “valid”.

4.1.1 Number of Estimations

In the satellite system-based evaluation, the following results have been obtained regarding the number of estimates:

- For the receiver CHC1, 208 out of 430 estimates are valid (48.4%), while for CHC2, 244 out of 425 estimates are valid (57.4%). For the smartphone SP01, 74 out of 164 estimates are valid (45.1%), and for SP02, 96 out of 213 estimates are valid (45.1%).

- The valid estimation rate for the geodetic receiver CHC1 was 43.2% on the first day, 50.7% on the second day, and 51.0% on the third day. These rates for CHC2 were 48.5%, 58.0%, and 64.9% respectively. The lower valid estimation rate for CHC1 on the first day can be explained by the AGP of the geodetic receiver. AGP is generally designed to provide maximum gain from the overhead direction and minimum gain from the horizon for the geodetic receivers. On the first day of the experiment, the receiver platform had a positive 20% incline, so the high-gain direction of CHC1's antenna was directed away from the 160° azimuth aligned with the experimental setup. This situation led to multipath effects being received with lower gain and caused a decrease in the number of valid estimates for GNSS-IR. The difference between valid estimation rates on the second and third days, where CHC1 receiver platform was negatively inclined and flat, was only 0.3%. Since the elevation angle range of 5°-25° was used for all days, it is understandable that there was no significant difference in the valid estimation rate between the last two days. The highest valid estimation rate for CHC2 was recorded on the last day at 64.9%. Generally, CHC2 has shown superiority over CHC1 in terms of the number of estimates and valid estimation rates.

- For the smartphone SP01, there was no valid estimate during the last three hours of the second day due to data interruption. When other periods were examined, the highest number of estimates was provided by GPS satellite system data, followed by Galileo and BeiDou systems.

- On the first day of the experiment with the smartphone SP01, no estimates were obtained from GLONASS data; on the second day from BeiDou and GLONASS data; and on the third day from Galileo satellites. In the smartphone SP02, no data was obtained from the GLONASS satellite on all three days of the experiment. This issue is thought to be due to software or hardware problems within the smartphone.

- For both SP01 and SP02, the most stable data obtained with GPS, and in terms of GNSS-IR valid estimation numbers, BeiDou system data followed GPS. However, for the Galileo system, although the number of estimates was high, the valid estimation rate was considerably low (17.1% for SP01 and 25.6% for SP02).

4.1.2 PBNR Values

In GNSS-IR analyses, the PBNR value is a commonly used quality control criterion. A high PBNR value indicates the presence of a regular reflection effect. In the satellite system-based evaluation, the following results have been obtained regarding PBNR values:

- For the receiver CHC1, the lowest PBNR values were obtained on the first day of the experiment, while the highest PBNR values were recorded on the second day. Considering that the receiver platform was positively inclined on the first day and negatively inclined on the second day and taking into account the AGP of the geodetic receivers, it can be said that the results match expectations. A similar situation applies to the receiver CHC2, which, being installed opposite to the zenith direction, shows an inverse correlation with the AGP effect compared to CHC1. According to the results, for CHC2, PBNR values of 11.7 and 10.5 were obtained on the first day, and 6.1 and 5.8 on the second day, for first 3-h and last 3-h periods, respectively. The orientation of CHC2, facing the same direction as the experimental setup on the first day and the opposite direction on the second day at a specific incline, resulted in higher PBNR values on the first day.

- When considering valid estimates from the geodetic receivers CHC1 and CHC2, the system providing the highest average PBNR value is Galileo, followed by GPS, GLONASS, and BeiDou.

- The PBNR values obtained for the smartphones SP01 and SP02 indicate that positioning the smartphones towards or away from the zenith direction has a weak impact on PBNR values. Similarly, it has been observed that the incline given to the platform does not significantly affect the PBNR values of the data.

4.1.3 Reflector Height Estimations

After the evaluation of PBNR values, the following results have been obtained for reflector height estimates in a satellite system-based assessment:

- For the CHC1, reflector height estimates on the first day showed errors of -4.1 cm and -6.2 cm, on the second day -4.2 cm and -2.5 cm, and on the last day -6.4 cm and -4.8 cm. The unidirectional nature of the errors suggests a negative bias in the estimates, which could be attributed to changes in terrain slope and surface roughness.

- The standard deviations of reflector height estimates with the CHC1 receiver were 8.2 cm and 6.7 cm on the first day, 4.9 cm and 5.6 cm on the second day, and 6.1 cm on both periods of the third day. The best standard deviation value was achieved on the second day when the antenna orientation was towards the 160° azimuth directed by the experimental setup, while the highest standard deviations over the three days occurred on the first day when the receiver's orientation was opposite to the setup. The results support the suitability of tilting the receiver platform toward the direction of interest on the terrain surface for GNSS-IR studies.

- Negative errors were also found in the reflector height estimates with the CHC2. Especially in the first periods, biases of -4.8, -3.2, and -6.1 cm were observed. In the second periods, positive errors of 0.8, 6.2, and 1.0 cm were seen from the first to the third day. However, looking at the standard deviations of the estimates, especially on the second and third days in the second periods, high values are observed. The value on the second day was 17.9 cm, and on the third day, it was 13.2 cm. Thus, it is difficult to assert a positive bias in the second period measurements. However, since the standard deviation values are lower in the first period measurements (respectively 4.5 cm, 9.4 cm, and 7.3 cm) and consistent results were obtained with CHC1, a negative bias can be claimed. The most precise results with CHC2 were obtained on the first day of the experiment, largely due to the AGP effect of the receiver.

- There were no significant differences in the performance of the satellite systems for reflector height estimates with CHC1. However, in CHC2, especially on the second day measurements, errors reaching up to 45 cm were observed in Galileo and GLONASS estimates. The increase in error amounts in the estimates obtained from CHC2 data in the second period measurements is due to the receiver being much closer to the ground than CHC1, thereby reducing the number of waves in the SNR data compared to data from CHC1 and decreasing the spectral resolution. The reduction in the number of complete waves lowers the spectral resolution, which in turn reduces the precision of the estimated frequency and thus the reflector height.

- On the smartphone SP01, a data interruption occurred during the second period of the second day. The sensitivity of the measurements in the first period of the second day was also lower compared to other days. While the reflector height estimation error on the second day's first period measurements was 32.6 cm, the standard deviation of the estimates was 16.6 cm. The number of estimates is significantly lower than first period of the first and third days. On the first day, the first period had 14 valid estimates, on the third day 20, while on the second day, the first period had only 6. Therefore, the statistical reliability of SP01's second day first period measurements is low. Consequently, this period will be excluded in evaluating performance of SP01.

- Examining the estimates from SP01 on the first and third days, the estimation errors are seen to be negatively directed. Errors on the first day were -4.0 cm and -6.1 cm, and on the second day -5.7 and -6.2 cm. There is also observed to be a negative bias in the estimates made with SP01 data. Therefore, the possibility that the negative bias in CHC1 estimates is receiver-induced is low. These errors are thought to stem from the surface characteristics of the terrain. Negative errors in SP02 estimates are only seen on the first day and the first period of the third day.

- It has been observed that the most stable data on the smartphones SP01 and SP02 is provided by GPS satellites. The largest data gap occurs in GLONASS satellite data. Data interruptions in Galileo and BeiDou signals have also been noted on the second day. Considering that geodetic receivers were able to collect a sufficient amount of data from various systems at the same times and days, these problems are thought to stem from the software and hardware characteristics of the smartphones.

Figure 5 shows the estimation errors and the standard deviations of estimates made with both the receivers and smartphones. Particularly, the CHC2 has been observed to provide estimates with high standard deviations during the second period measurements. The CHC1 has provided the most stable estimates in the first period measurements. The performance of the smartphone SP01, when excluding the second day, is close to that of CHC1. Overall, it has been observed that reflector height estimation with an accuracy of 5-10 cm can be achieved using both geodetic receivers and smartphones with standard setups.

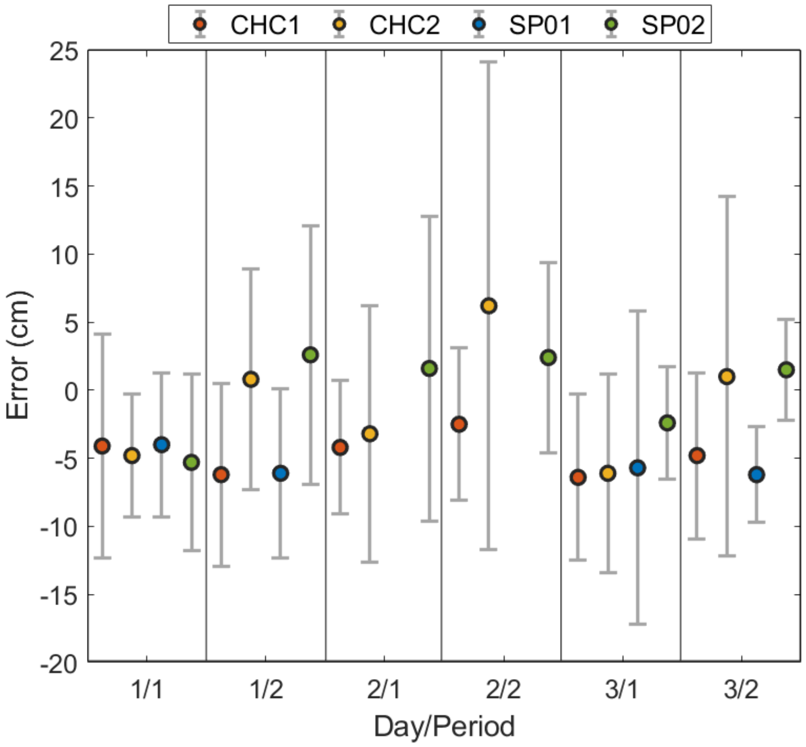

Figure 5: *Errors of reflector height estimations with geodetic receivers and smartphone data on different days and periods*

4.1.4 Reflector Height Change Estimations

One of the most significant outcomes of this study is the estimation of height changes. This is crucial because long-term monitoring of climatic parameters such as snow depth and sea level relies on revealing their temporal changes, i.e., determining height variations. In this study, a height change of 10 cm between two periods was planned. However, the application of this value varied on some days during fieldwork and in the experimental setup. The height change measured on the first day was 9.0 cm and 10.5 cm on subsequent days for the receiver named CHC1, while for CHC2, it was 4.5 cm on the first day, 12.0 cm on the second day, and 10.5 cm measured on subsequent days. For the receivers SP01 and SP02, except for the second day when data interruption occurred in SP01, a height change of 10 cm was successfully applied each day.

Height change estimates made with the receiver named CHC1, when evaluated collectively across all satellite systems, were obtained as 11.1 cm on the first day, 8.0 cm on the second day, and 8.9 cm on the third day. Except for estimates made with BeiDou data on the first day, GLONASS data on the second day, and Galileo data on the third day, a 10 cm height change was determined with estimation errors below 3 cm. However, estimates with CHC2 contain significant errors. Particularly on the second day, the high standard deviations of the reflector height estimations also affected the accuracy of the height differences. Some systems provided results close to the in-situ values on different days of the experiment. For example, the height change estimate made with BeiDou data on the first day is 4.7 cm, while the in-situ value that day is 4.5 cm. It is evident from the results that the satellite system-based classification was not sufficient to separate good and bad signals for the receiver named CHC2. A frequency-based evaluation might be more suitable for this receiver configuration.

Estimations obtained with data from the smartphone SP01 were found as 12.1 cm on the first day and 10.5 cm on the third day. For SP02, the estimates were 2.1 cm on the first day, 9.2 cm on the second day, and 6.1 cm on the third day. The errors in the estimates made with SP02 data, compared to SP01, could be due to it being closer to the ground, which reduces the spectral resolution in frequency estimation, and possible reflections or signal interferences from the experimental setup and receivers mounted on it. To mitigate these potential causes, further studies could place smartphones and receivers on separate setups without any physical connection between them.

4.2 Frequency Based Assessment

The receivers and smartphones used in the study have the capability to collect signals at different frequencies. Different frequencies can be distinguished by their sensitivity to multipath effects and their reflection characteristics. Therefore, a frequency-based analysis is necessary to evaluate the performance of various frequencies. The types of signals, frequency bands, frequencies, and wavelengths that geodetic receivers and smartphones can collect are provided in Table 3. In the table, “k” represents the GLONASS frequency channel, which varies between -7 and +12.

Table 3: *Supported signals, frequency bands, frequencies and wavelengths for geodetic receivers and smartphones used*

Satellite System	Signal Type	Frequency Band	Frequency (MHz)	Wavelength (cm)	CHC#	SP##
GPS	S1C	L1	1575.42	19.03	+	+
	S2P	L2	1227.60	24.42	+	-
	S5X	L5	1176.45	25.48	+	+
GLONASS	S1C	G1	1602+k x 9/16	18.64-18.76	+	+
	S2P	G2	1246+k x 7/16	23.96-24.12	+	-
Galileo	S1X	E1	1575.42	19.03	+	-
	S5X	E5a	1176.45	25.48	-	+
	S8X	E5 (E5a+E5b)	1191.795	25.15	+	-
BeiDou	S1I	B1	1561.098	19.20	+	-
	S2I	B1-2	1561.098	19.20	-	+
	S6I	B3	1268.52	23.63	+	-

Since observations on the same frequency but different signal types are found in both receivers and smartphones and considering that signal frequency is one of the most crucial parameters affecting surface reflection, different signal types have been grouped under two categories. Since frequency is inversely proportional and directly related to wavelength, the grouping has been based on wavelength. Therefore, frequency bands with wavelengths shorter than 20 cm and those longer than 20 cm have been categorized as follows, and the results have been derived based on these groups:

- **Frequency Group 1 (FG1):** GPS S1C, GLO S1C, GAL S1X, BDS S1I, and BDS S2I.
- **Frequency Group 2 (FG2):** GPS S2P, GPS S5X, GLO S2P, GAL S5X, GAL S8X, BDS S6I.

4.2.1 Number of Estimation

The number of estimates in Frequency Groups 1 and 2, abbreviated as FG1 and FG2, has been determined separately for each receiver and smartphone. Table 4 presents the number of estimates derived from data collected by the receivers and smartphones.

Table 4: *Number of estimations for data at different frequencies collected by geodetic receivers and smartphones*

			Day 1		Day 2		Day 3	
Receiver	**Frequency Group**	**Data type**	**First 3-h**	**Last 3-h**	**First 3-h**	**Last 3-h**	**First 3-h**	**Last 3-h**
CHC1	FG1	All	26	37	26	41	30	36
		Valid	11	14	11	20	14	19
	FG2	All	32	44	32	47	38	41
		Valid	16	19	19	24	19	22
CHC2	FG1	All	25	36	25	41	30	37
		Valid	12	19	14	23	18	24
	FG2	All	31	42	31	46	38	43
		Valid	17	17	20	26	24	30
SP01	FG1	All	23	28	14	5	24	24
		Valid	13	15	6	-	18	18
	FG2	All	11	13	7	1	9	5
		Valid	1	1	-	-	2	-
SP02	FG1	All	24	28	19	27	24	21
		Valid	13	18	12	18	14	14
	FG2	All	11	14	9	14	11	11
		Valid	3	1	-	2	1	-

According to Table 4, for the geodetic receivers CHC1 and CHC2, the number of estimates in FG2 is higher than in FG1. For the smartphones SP01 and SP02, it has been observed that there are twice as many or more estimates in FG1 compared to FG2. In the smartphone SP01, nearly all valid estimates are obtained with data from FG1. Data from FG2 provided only one valid estimate in each of the two periods on the first day and two valid estimates in the first period on the last day. For the smartphone SP02, FG1 has also emerged as prominent in frequency-based evaluation. Due to the insufficient number of estimates in FG2, its usability in GNSS-IR studies is limited.

4.2.2 PBNR Values

When evaluating different frequency groups in terms of PBNR, it has been observed that geodetic receivers and smartphones produce contrasting results. Accordingly, in geodetic receivers, higher PBNR values are obtained in FG2 compared to FG1, while in smartphones, FG1 yields higher values than FG2. In smartphone data, the PBNR values of data in FG1 are approximately twice those in FG2.

4.2.3 Reflector Height Estimations

Reflector height estimates and standard deviation values obtained from data collected at different frequencies from geodetic receivers and smartphones are provided in Table 5. Values obtained without applying conditions are labeled as “all”, while values obtained when conditions are applied are labeled as “valid”. The values in parentheses represent standard deviations in centimeters.

Table 5: *Reflector height estimations and their standard deviations using geodetic receivers and smartphone data at different frequencies (reflector heights in m, standard deviations in cm)*

			Day 1		Day 2		Day 3	
Receiver	**Frequency Group**	**Data type**	**First 3-h**	**Last 3-h**	**First 3-h**	**Last 3-h**	**First 3-h**	**Last 3-h**
CHC1	FG1	All	1.852 (111.1)	2.317 (124.5)	2.416 (117.5)	2.037 (92.4)	2.080 (71.7)	2.293 (112.1)
		Valid	1.879 (8.1)	1.768 (4.8)	1.924 (3.9)	1.831 (4.4)	1.914 (5.4)	1.827 (5.4)
	FG2	All	1.973 (113.7)	2.266 (124.1)	1.892 (70.1)	2.307 (114.9)	2.050 (91.0)	2.129 (97.8)
		Valid	1.863 (8.5)	1.751 (7.9)	1.922 (5.5)	1.839 (6.6)	1.936 (6.5)	1.845 (6.6)
CHC2	FG1	All	1.450 (107.9)	1.780 (131.0)	1.963 (151.7)	1.907 (150.9)	1.430 (107.3)	1.601 (132.9)
		Valid	1.063 (2.4)	1.068 (6.9)	1.071 (3.9)	0.985 (9.7)	1.091 (3.1)	0.984 (5.7)
	FG2	All	1.818 (142.5)	1.967 (138.6)	1.780 (136.1)	1.945 (142.8)	1.823 (137.0)	1.584 (111.9)
		Valid	1.104 (4.9)	1.130 (8.3)	1.127 (11.4)	1.158 (19.6)	1.122 (9.2)	1.149 (12.9)
SP01	FG1	All	2.457 (125.9)	2.464 (112.1)	2.344 (124.1)	2.104 (217.9)	2.107 (93.4)	2.227 (109.4)
		Valid	1.903 (5.5)	1.774 (4.9)	2.266 (16.6)	-	1.909 (6.0)	1.778 (3.5)
	FG2	All	2.092 (122.2)	2.361 (158.0)	2.822 (92.1)	0.007 (-)	2.512 (129.4)	2.234 (156.5)
		Valid	1.928 (-)	1.936 (-)	-	-	1.647 (25.3)	-
SP02	FG1	All	1.748 (153.1)	1.951 (140.4)	1.461 (90.8)	1.895 (133.2)	1.924 (145.3)	2.180 (153.9)
		Valid	1.184 (4.2)	1.180 (9.3)	1.256 (11.2)	1.149 (3.5)	1.220 (4.0)	1.155 (3.7)
	FG2	All	1.579 (133.3)	2.303 (171.5)	2.257 (136.0)	2.289 (150.1)	2.648 (147.3)	2.461 (194.7)
		Valid	1.308 (4.4)	1.299 (-)	-	1.301 (17.2)	1.165 (-)	-

For the CHC1 receiver, contrary to the number of estimates and PBNR values, more precise results have been obtained in reflector height estimates with data from FG1 compared to FG2. According to the Table 5, for a standard setup situation, it can be said that FG1 data provides better reflector height estimates compared to data from FG2. For the CHC2 receiver, using data from FG1 has significantly improved the quality of reflector height estimates. Therefore, whether the geodetic receiver is installed toward the zenith direction or its opposite, FG1 data is more suitable for GNSS-IR reflector height estimates than FG2 data.

Almost all valid estimates are obtained with data from FG1 with the smartphone SP01. Data from FG2 provided only one valid estimate in each of two periods on the first day and two valid estimates only in the first period on the last day. The standard deviation calculated from these two estimates on the last day is 25.3 cm, indicating that the usability of FG2 data in

GNSS-IR studies with smartphones appears limited. With FG1 data, reflector height estimates with standard deviation values below 6 cm have been achieved for the first and third days. For the smartphone SP02, FG1 has also emerged as prominent in frequency-based evaluation. The insufficient number of estimates in FG2 and the low accuracy of the few estimates it provides limit its usability in GNSS-IR studies. Using only FG1 signals provided better results compared to using all signals. When all signals were used, the standard deviation value found was 6.5 cm on the first day of the first period, which decreased to 4.2 cm when only FG1 signals were used. These values were 7.0 cm when all signals were used and 3.5 cm when only FG1 signals were used on the second day of the second period.

4.2.4 Reflector Height Change Estimations

Estimations of reflector height changes and standard deviation values obtained from data collected at different frequencies from geodetic receivers and smartphones are given in Table 6. Here, the reflector height changes are calculated by subtracting two different reflector heights, so the errors in reflector heights propagate to the error in the change. In these values, only the results obtained when conditions were applied are presented, as values obtained without applying conditions were statistically insignificant.

Table 6: *Reflector height change estimations, their standard deviations, and in-situ measurements in cm units, obtained using geodetic receivers and smartphone data at different frequencies*

Receiver	Data Type	Day 1	Day 2	Day 3
CHC1	In-situ	9.0	10.5	10.5
	FG1	11.1 (9.4)	9.3 (5.9)	8.7 (7.6)
	FG2	11.2 (11.6)	8.3 (8.6)	9.1 (9.3)
	All	11.1 (10.6)	8.8 (7.4)	8.9 (8.6)
CHC2	In-situ	4.5	12.0	10.5
	FG1	-0.5 (7.3)	8.6 (10.5)	10.7 (6.5)
	FG2	-2.6 (9.6)	-3.1 (22.7)	-2.7 (15.8)
	All	-1.1 (9.3)	2.6 (20.2)	3.4 (15.1)
SP01	In-situ	10.0	9.5	10.0
	FG1	12.9 (7.4)	-	13.1 (6.9)
	FG2	-0.8 (-)	-	-
	All	12.1 (8.2)	-	10.5 (12.0)
SP02	In-situ	10.0	10.0	10.0
	FG1	0.4 (10.2)	10.7 (11.7)	6.5 (5.4)
	FG2	0.9 (4.4)	-	-
	All	2.1 (11.5)	9.2 (13.2)	6.1 (5.5)

Using signals from FG1 in reflector height change estimations with the CHC1 receiver has shown improvement. The standard deviations of height change estimations decreased from 10.6 cm to 9.4 cm on the first day, from 7.4 cm to 5.9 cm on the second day, and from 8.6 cm to 7.6 cm on the third day.

As mentioned in the satellite-based evaluation, it has not been possible to accurately estimate the applied height changes in the field using all signals or when evaluating different satellite systems separately in CHC2 data. However, after grouping the same data into FG1 and FG2, it has been observed that the height changes on the second and third days could be obtained with estimation errors below 3.5 cm using FG1 signals. On the second day, the height change of 12 cm was estimated at 8.6 cm, and on the third day, the height change of 10.5 cm was estimated at 10.7 cm. Height changes found with FG2 signals are not significant. Therefore, it can be said that using signals from FG1 in GNSS-IR studies is appropriate for the CHC2 receiver.

In reflector height change estimations made with data from the smartphones SP01 and SP02, signals from FG1 have been dominant. For SP01, height change estimations using FG1 data are 12.9 cm and 13.1 cm on the first and third days, respectively. For SP02, these values are 0.4 cm on the first day, 10.7 cm on the second day, and 6.5 cm on the third day. For both smartphones, the standard deviations of height change estimations are lower when using FG1 signals compared to when using all signals.

5. Conclusion

In this study, the performance of determining SNR metrics through the analysis of multi-GNSS and multi-frequency SNR data provided by geodetic receivers and Android-based smartphones at different platform inclinations has been comparatively examined. The results from this 3-day experiment have been evaluated in terms of satellite systems and signal frequencies.

Initially, it was observed that the CHC2 receiver provided a higher number of estimates and a higher valid estimate rate compared to the CHC1 receiver. Similarly, higher average PBNR values were obtained with CHC2 compared to CHC1. For smartphones SP01 and SP02, PBNR values were found to be similar, indicating that platform orientation had a weak impact on PBNR values. The inclination of the platform also did not affect the PBNR values for smartphone data. Therefore, depending on the goals of future studies, smartphones can be mounted on flat, inverted, or inclined platforms. The setup does not significantly affect GNSS-IR performance. In reflector height estimations, no significant performance variation dependent on the satellite system was observed for data from the CHC1 receiver. However, in CHC2, errors up to 45 cm were seen with Galileo and GLONASS data on the second day. For smartphones, the most stable data was collected from GPS satellites, with interruptions in Galileo and BeiDou signals observed on the second day.

The 10 cm height change applied to the setup was determined with estimation errors below 3 cm using CHC1. Height change estimates with SP01 and SP02 data varied, with SP02 showing larger errors due to lower spectral resolution and possible signal interferences. To mitigate these issues, future studies could mount smartphones and receivers on separate setups without any physical connection between them. In the frequency-based evaluation, frequencies shorter and longer than 20 cm have been included in FG1 and FG2, respectively, and evaluations have been conducted considering these two groups. It has been observed that geodetic receivers and smartphones produce contrasting results. In geodetic receivers, FG2 provided higher number of estimates and PBNR values than FG1, while in smartphones, FG1 was found to be better.

Reflector height estimations with FG1 data were more precise than those with FG2 data. For CHC2, FG1 data significantly improved reflector height estimations. Based on the results, it is not recommended to use FG2 data when the receiver is set up to face opposite to the zenith direction. In smartphone data, almost all estimates are obtained with FG1 data. The usability of FG2 data in GNSS-IR studies with smartphones is weak due to low number of estimates and accuracy. According to the results, evaluating only FG1 signals instead of all signals in smartphone data has improved the accuracy of the estimates. Using FG1 signals also improved reflector height change estimations with CHC1, reducing estimation errors and standard deviation values. Statistically significant height changes were observed with FG1 signals for CHC2 after frequency-based classification, while FG2 signals proved less meaningful. For smartphones, FG1 data provided better standard deviations compared to using all signals.

Overall, the main outcomes of the study can be summarized as follows:

- Geodetic receivers are more consistent in data collection compared to smartphones.

- Mounting smartphones on flat, inverted, or inclined platforms has a weak effect on GNSS-IR estimations.
- The most stable data in smartphones is obtained from GPS satellites.
- Using signals with wavelengths shorter than 20 cm in GNSS-IR studies involving smartphones provides better results compared to using all signals.
- Both geodetic receivers and smartphones can be used for detecting reflector height and height changes, and for long-term monitoring.
- The usability of smartphone data for determining reflector height changes highlights a cost-effective alternative for monitoring climatological parameters such as snow depth, sea level, and vegetation height using GNSS-IR. Given their significantly lower cost compared to geodetic receivers, smartphones offer a practical alternative in such studies.

Acknowledgements

This study was conducted as part of the doctoral thesis being prepared by the first author at Yildiz Technical University, Graduate School of Science and Engineering, Department of Geomatic Engineering. And, the study has been supported by the Scientific and Technological Research Council of Türkiye (TÜBİTAK) within the scope of the Research Support Projects Directorate (ARDEB) under project number 121Y348.

Author Contribution

Cemali Altuntas: Conception, Design, Methodology, Literature review, Analysis, Software, Data collection and processing, Writing. **Nursu Tunalioglu:** Conception, Design, Methodology, Supervision, Analysis, Writing.

Declaration of Competing Interests

The authors declare that they have no known relevant competing financial or non-financial interests that could have appeared to influence the work reported in this paper.

References

Altuntas, C., & Tunalioglu, N. (2020). Estimation performance of soil moisture with GPS-IR method. *Sigma Journal of Engineering and Natural Sciences*, *38*(4), 2217-2230.

Altuntas, C., & Tunalioglu, N. (2021). Feasibility of retrieving effective reflector height using GNSS-IR from a single-frequency android smartphone SNR data. *Digital Signal Processing*, *112*, 103011.

Altuntas, C., Iban, M. C., Şentürk, E., Durdag, U. M., & Tunalioglu, N. (2022). Machine learning-based snow depth retrieval using GNSS signal-to-noise ratio data. *GPS Solutions*, *26*(4), 117.

Altuntas, C., & Tunalioglu, N. (2023). A systematic approach for identifying optimal azimuth and elevation angle masks in GNSS-IR: validation through a sea level experiment. *GPS Solutions*, *27*(4), 198.

Banville, S., & van Diggelen, F. (2016). Precise positioning using raw GPS measurements from Android smartphones, *GPS World*, *27*(11), 43-48.

Besel, C., & Kayikci, E. T. (2021). Investigation of sea level variations in Turkish coasts using GNSS reflectometry (in Turkish). *Journal of Geodesy and Geoinformation*, *8*(1), 1-17.

Chen, L., Chai, H., Zheng, N., Wang, M., & Xiang, M. (2023). Feasibility and performance evaluation of low-cost GNSS devices for sea level measurement based on GNSS-IR. *Advances in Space Research, 72*(11), 4651-4662.

Chew, C. C., Small, E. E., Larson, K. M., & Zavorotny, V. U. (2013). Effects of near-surface soil moisture on GPS SNR data: Development of a retrieval algorithm for soil moisture. *IEEE Transactions on Geoscience and Remote Sensing*, *52*(1), 537-543.

EUSPA. (2024). *EUSPA EO and GNSS Market Report, Issue 2*. Publications Office of the European Union, Luxembourg.

GSA. (2019) *GNSS Market Report, Issue 6*. Publications Office of the European Union, Luxembourg.

Hu, Y., Yuan, X., Liu, W., Wickert, J., Jiang, Z., & Haas, R. (2021). GNSS-IR model of sea level height estimation combining variational mode decomposition. *IEEE Journal of Selected Topics in Applied Earth Observations and Remote Sensing*, *14*, 10405-10414.

Larson, K. M., Small, E. E., Gutmann, E. D., Bilich, A. L., Braun, J. J., & Zavorotny, V. U. (2008). Use of GPS receivers as a soil moisture network for water cycle studies. *Geophysical Research Letters*, *35*(24).

Larson, K. M., Gutmann, E. D., Zavorotny, V. U., Braun, J. J., Williams, M. W., & Nievinski, F. G. (2009). Can we measure snow depth with GPS receivers?. *Geophysical research letters*, *36*(17).

Larson, K. M., Löfgren, J. S., & Haas, R. (2013). Coastal sea level measurements using a single geodetic GPS receiver. *Advances in space research*, *51*(8), 1301-1310.

Larson, K. M., & Nievinski, F. G. (2013). GPS snow sensing: results from the EarthScope Plate Boundary Observatory. *GPS Solutions*, *17*, 41-52.

Liu, Z., Du, L., Zhou, P., Liu, Z., Zhang, Z., & Xu, Z. (2022). Performance assessment of GNSS-IR altimetry using signal-to-noise ratio data from a Huawei P30 smartphone. *GPS Solutions*, *26*(2), 42.

Lomb, N. R. (1976). Least-squares frequency analysis of unequally spaced data. *Astrophysics and space science*, *39*, 447-462.

Nievinski, F. G., & Larson, K. M. (2014). Inverse modeling of GPS multipath for snow depth estimation—Part II: Application and validation. *IEEE transactions on geoscience and remote sensing*, *52*(10), 6564-6573.

Robustelli, U., Baiocchi, V., & Pugliano, G. (2019). Assessment of dual frequency GNSS observations from a Xiaomi Mi 8 Android smartphone and positioning performance analysis. *Electronics*, *8*(1), 91.

Scargle, J. D. (1982). Studies in astronomical time series analysis. II-Statistical aspects of spectral analysis of unevenly spaced data. *Astrophysical Journal*, *263*, 835-853.

Strandberg, J., & Haas, R. (2019). Can we measure sea level with a tablet computer?. *IEEE Geoscience and Remote Sensing Letters*, *17*(11), 1876-1878.

Tunalioglu, N., Dogan, A. H., & Durdag, U. M. (2019). Determination of snow depth by GPS signal to noise ratio (in Turkish). *Journal of Geodesy and Geoinformation*, *6*(1), 1-9.

Williams, S. D., Bell, P. S., McCann, D. L., Cooke, R., & Sams, C. (2020). Demonstrating the potential of low-cost GPS units for the remote measurement of tides and water levels using interferometric reflectometry. *Journal of atmospheric and oceanic technology*, *37*(10), 1925-1935.

Zheng, N., & Chai, H. (2023). Preliminary inquiry on the linear relationship between the height of the station and the ground height error retrieved by GNSS-IR with low-cost smart electronic equipment. *Measurement Science and Technology*, *34*(12), 125115.